

Spectroscopy of Giant Colloidal Crystals

Tsuneo OKUBO* and Akira TSUCHIDA

Department of Applied Chemistry, Gifu University, Gifu 501-1193, Japan

**E-mail address: okubotsu@apchem.gifu-u.ac.jp*

(Received May 9, 2002; Accepted June 14, 2002)

Keywords: Colloidal Crystal, Reflection Spectra, Electrical Double Layer, Crystallization, Electro-Optic Effect

Abstract. Colloidal crystals are the suspensions in which colloidal particles distribute regularly as atoms and molecules do in metals and protein crystals. Giant colloidal crystals invented by the authors emit brilliant iridescent light by the Bragg diffraction and are quite beautiful. In this article recent works in our laboratory on the spectroscopic study of the crystallization kinetics, structural and dynamic properties and the electro-optic effects of giant colloidal crystals have been discussed. Formation of giant colloidal single crystals is due to the electrostatic intersphere “repulsion” and to the highly expanded electrical double layers surrounding colloidal spheres. Spectroscopic measurements, e.g., transmitted light spectrum, reflection spectrum and static and dynamic light scattering reveals the importance of the electrical double layers for colloidal crystallization. The substantial acceleration effect of microgravity in the alloy crystallization supports that the colloidal crystallization takes place by the condition whether the maximum packing density is achieved or not for a given ratio of the sphere sizes including surrounding electrical double layers.

1. Introduction

Colloidal suspensions display extraordinary structures in particle distributions, “gas”, “liquid” and “crystal” structures, especially in deionized suspensions (PIERANSKI, 1983; OKUBO, 1988, 1993a; OTTEWILL, 1989; RUSSEL *et al.*, 1989). Suspensions showing crystal structures are named as colloidal crystals and are ideal for model studies of metals and protein crystals, since the colloidal structures are analyzed much conveniently with optical techniques and even with the naked eye. A study of the colloidal crystals is also helpful in understanding the fundamental properties of states of substances, phase transition, and electrostatic interactions of macroionic systems. Two essentially important factors causing the colloidal crystals are the Brownian movement of spheres and an electrostatic intersphere repulsion accompanied with the expanded electrical double layers around the spheres especially in the deionized state.

It should be mentioned here that Ise *et al.* has proposed the interparticle “attraction” (not “repulsion”) as the important interaction for colloidal crystallization for more than ten

years (OKUBO, 1988). However, their idea is completely wrong and must be discarded. Quite recently, they withdrew their idea in their own paper, and supported “repulsion”, including the Alder transition and Yukawa potential instead (SHINOHARA *et al.*, 2001).

The thickness of the electrical double layers is approximated by the Debye screening length, l_{DH} :

$$l_{\text{DH}} = (4\pi e^2 n / \epsilon k_{\text{B}} T)^{-1/2},$$

where e is the electronic charge, ϵ is the dielectric constant of the solvent, k_{B} is the Boltzmann constant, T is the absolute temperature and n is the concentration of “diffusible” or “free-state” cations and anions in suspension. Thus, n is the sum of the concentrations of diffusible counterions, foreign salt and both H^+ and OH^- from the dissociation of water. Note that the maximum value of l_{DH} observed for the exhaustively deionized suspension is *ca.* $1 \mu\text{m}$ in water, which is estimated by taking $n = 2 \times 10^{-7} (\text{mol dm}^{-3}) \times N_{\text{A}}$ (Avogadro’s number) $\times 10^{-3} \text{ cm}^{-3}$, and large compared with the size of the typical colloidal particles. Colloidal crystallization is nicely explained with the *effective soft-sphere* model. The effective diameter, d_{eff} , of spheres includes l_{DH} , and is given by the diameter plus twice the Debye length. When d_{eff} is shorter than the observed intersphere distance, l , a gas-like distribution is observed. When d_{eff} is comparable to, or a bit shorter than the intersphere distance, the distribution of spheres is usually liquid. When d_{eff} is close to, or larger than the observed intersphere distance, crystal ordering is formed. This effective soft-sphere model was supported by systematic comparison between d_{eff} and l values (OKUBO, 1988, 1993a).

2. Giant Colloidal Crystals

The iridescent colors and single crystals are most beautiful and attractive. Colloidal crystals are surrounded by grain boundaries and are quite similar to metals. The iridescent colors are ascribed to the Bragg diffraction of visible light by the lattice planes of the colloidal crystals. Lattice spacing of the colloidal crystals is several thousands larger than that of metals and is in the range of light wavelengths. Very little work has been reported on the morphology, e.g., shape and size, of the colloidal single crystals, since the size of the crystals is very small, in the order of several hundred micrometers even for the largest ones. The main reason for the scarcity of the work is the fact that it had been very difficult to obtain completely deionized suspensions, which contain the charges from the particles and their counterions. In order to obtain the completely deionized suspension, highly effective mixed beds of cation- and anion-exchange resins such as Bio-Rad resins have to coexist in suspension for a long time, more than 3 years. From our experiences, the deionization process of suspension with resins is unexpectedly slow. This may be due to the fact that the deionization reaction takes place between solid (colloidal particles) – solid (resins) phases via liquid medium (water). It is interesting to note that the colloidal crystallization takes place at the very low particle concentrations for the deionized suspension. Spectroscopic studies of the deionized suspensions in non-aqueous media have been studied (PUSEY and VAN MEGEN, 1986; OKUBO, 1990a, 1992a, 1994a; OKUBO *et al.*,



Fig. 1. A close-up photograph of the colloidal single crystals of silica spheres (103 nm in diameter) in a plate cell. $\phi = 0.000952$. With ion-exchange resins, 7 days after suspension preparation, 40 min after inverted mixing. Exposure = 2 s, iris = 22 (taken from OKUBO, 1994c).

2002). However, critical concentrations of melting are high compared with those in aqueous systems, and single crystals in non-aqueous media are very small in most cases.

About ten years ago, Okubo succeeded to have very large single crystals, 2–8 mm in size in a test tube of 13 mm in outside diameter (OKUBO, 1992a, 1993b, 1994a, b). Figure 1 shows a close-up photograph of single crystals appearing in an aqueous dispersion of silica spheres, 103 nm in diameter. The cell used was a quartz glass optical cell for fluorescence measurements, 10 mm in width, 10 mm in depth and 70 mm in height. In the

bottom of the cell, the resins coexist, although a view of the bottom of the cell is omitted here. The photograph was taken 7 days after suspension preparation, and 40 h after inverted mixing. The stock suspension of spheres was deionized with Bio-Rad resins more than 3 years. The sphere concentration was 0.000952 in volume fraction. Under these experimental conditions, only a very few nuclei are formed and large single crystals are formed. There are two kinds of single crystals observable in the photograph. Block-like crystals are formed by the homogeneous nucleation mechanism in the bulk phase far from the cell wall. Pillar-like crystals grow by the heterogeneous nucleation mechanism along the cell wall. The colors of the crystals changed as the angle of the light source and/or camera changed, which is clearly due to the change in the Bragg diffraction wavelength. Size of the single crystals is very large at the sphere concentration slightly higher than the critical concentration of melting (OKUBO, 1994a, b).

3. Principle of Transmitted-Light and Reflection Spectroscopy

Transmitted-light and reflection spectrophotometry is quite effective in analyzing the lattice structure of colloidal crystals, since the Bragg diffraction wavelength locates in the range of visible wavelength (OKUBO, 1986a, b, c). When the scattering angle (2θ) is 180° for the transmitted light spectrum measurements, the absorption peak wavelength λ_{\max} is given by:

$$\lambda_{\max}/n_s = 2d\sin\theta = 2d$$

where d denotes the Bragg length and n_s is the refractive index of the sample suspension. For both face-centered (fcc) and body-centered (bcc) cubic lattices, the nearest-neighbored intersphere distance (l_f or l_b , respectively) is given for the transmitted-light by:

$$l_f (=l_b) = (3/2)^{1/2}d = 0.6124(\lambda_{\max}/n_s).$$

For the reflection spectroscopy, the interparticle distance for the plate cell is given by:

$$l_f (=l_b) = (3/8)^{1/2} \times [\lambda_{\max}^2/(n_s^2 - n_a^2 \cos^2\theta)^{1/2}]$$

where n_a designates the refractive index of air. The nearest-neighbored intersphere distance (l_f or l_b), the Bragg distance (d_f or d_b) and the lattice constant (a_f or a_b) are given as:

$$(l_f/0.707) = 3^{1/2}d_f = a_f$$

$$(l_b/0.866) = 3^{1/2}d_b = a_b.$$

Subscripts f and b denote the fcc and bcc lattices, respectively. From these equations the ratio d_f/d_b (or a_f/a_b) is derived as:

$$d_f/d_b = l_f/l_b = 1.0284.$$

The fcc lattice structure is more stable than the bcc, and the former is formed favorably at high sphere concentration, at low suspension temperature and at low salt concentration. When two lattices coexist, reflection pattern is a double peak, with a difference of 1.03 in the ratio of the wavelengths of the two peaks.

4. Elastic Properties of Colloidal Crystals

Elastic moduli of colloidal crystals are very small, of the order 10^{-2} – 10^3 Pa, whereas those of metals are in the range of 10^{10} – 10^{12} Pa. Thus, a colloidal crystal is distorted very easily by weak external field, such as gravitational field, shearing forces, an elevated pressure, an electric field, centrifugal compression, and so on. From the concentration dependence of the intersphere distance, l , in the bottom layer, the static elastic modulus can be determined at sedimentation equilibrium using ultramicroscopic technique. Furthermore, from the height dependence of the intersphere distance at a sedimentation equilibrium, elastic moduli were determined (OKUBO, 1989) from the reflection spectroscopy by:

$$l - l_m = (\rho_{\text{eff}} g_0 D_m \phi_m / G)(h - h_m),$$

where h and h_m are the heights of the horizontal planes examined and the horizontal midplane of the colloidal suspension in the cell, respectively, ρ_{eff} is the effective density given by the specific gravity of the spheres minus that of solvent, g_0 is the gravitational constant, and G the rigidity. The elastic properties are summarized as follows (OKUBO, 1987, 1988, 1989, 1990a; OKUBO and ISHIKI, 2001). Firstly, $\log G$ increased linearly with a slope of unity, as $\log N$ (sphere concentration, number per unit volume) increased. This relationship holds since the rigidity of colloidal crystal is given by the force constant divided by the intersphere distance (l), and then given by the number density, N times $k_B T$ and divided by the square of the thermal fluctuation parameter, g :

$$G \propto f/l \propto (k_B T / \langle \delta^2 \rangle) / l \propto N k_B T / g^2.$$

Secondly, the elastic moduli were larger than those of colloidal liquid when comparison was made at the same sphere concentration. Thirdly, rigidity of colloidal crystals increased sharply as the deionization of the suspension proceeded.

Colloidal crystals in a rotating disk are also compressed in a centrifugal field (OKUBO, 1990b). Beautiful color bands appeared under the centrifugal field. The elastic moduli at various sphere concentrations have been measured from the change in the reflection peak wavelengths in the centrifugal equilibrium.

5. Structural Relaxation Time

Structural relaxation time (τ) of colloidal crystal was observed, for the first time, by the spectrophotometric and conductance stopped-flow techniques for the deionized spheres (35 to 2950 nm in diameter) (OKUBO, 1997a, b). Two kinds of τ values, fast (τ_f) and slow steps, are observed. The former is given by the simple relation:

$$\tau_r = \eta/G,$$

where η is the viscosity and G denotes the rigidity of latex suspension. The τ_r values decreased as sphere concentration increased. Theoretical values for τ_r , calculated using the translational diffusion constants of the spheres evaluated by the Einstein-Stokes equation, agreed nicely with the observed τ_r values. The results support strongly that the electrostatic intersphere repulsion is essential to explain the dynamic properties of colloidal crystal.

6. Melting Temperature and Refractive Index

The melting temperature, T_m of colloidal crystals has been measured by the reflection spectroscopy as a function of sphere concentration. T_m increased substantially as the deionization process of the suspension proceeded. The most reliable values of T_m observed for the completely deionized suspensions are successfully analyzed with the theory of Williams *et al.* (WILLIAMS *et al.*, 1976; OKUBO, 1991, 1992b), and values of the heat and entropy of melting were obtained. T_m values are consistent with the theory of Robbins *et al.*, which treats the repulsive Yukawa potential between colloidal spheres (ROBBINS *et al.*, 1988). Refractive indices of colloidal crystals and liquids were measured using a laser differential refractometer (OKUBO, 1990c).

7. Static and Dynamic Light-Scattering

Static (SLS) and dynamic light-scattering (DLS) measurements were made for colloidal crystals, liquids and gases in the exhaustively deionized suspension (OKUBO *et al.*, 1995, 1996; OKUBO and KIRIYAMA, 1997; OKUBO, 1997c).

Figure 2 shows the typical examples of SLS intensity, $I(q)$ and the effective diffusion coefficients, D_{eff} from DLS measurements as a function of a scattering vector, q . Circles and crosses indicate the data for the suspensions with and without resins coexisted. The suspensions are crystal and liquid, respectively. Surprisingly, very sharp peaks appeared for the crystals. The measurements have been made at intervals of half the degree! However, this interval was not always narrow enough for the determination of the reliable values of peak scattering vector, q_m . The nearest-neighbored interparticle distances of colloidal crystals and liquids estimated from the peaks in the structure factor $S(q)$ curves, l_{obs} agreed excellently with the effective diameters of spheres (d_{eff}) including the electrical double layers in the effective soft-sphere model and also with the mean intersphere distances, l_0 calculated from the sphere concentration ($l_{\text{obs}} \approx d_{\text{eff}} \approx l_0$). Three and two dynamic processes have been extracted separately from time profiles of autocorrelation function of colloidal crystals and liquids, respectively. Decay curves of colloidal gases are characterized by a single translational diffusion coefficient, D_0 . D_0 of the gases is always lower than the calculation from the Stokes-Einstein equation with the true diameter of spheres, and increases as ionic concentration increases. These experimental results emphasize the important role of the expanded electrical double layers on the diffusive properties for colloidal crystals, liquids and gases.

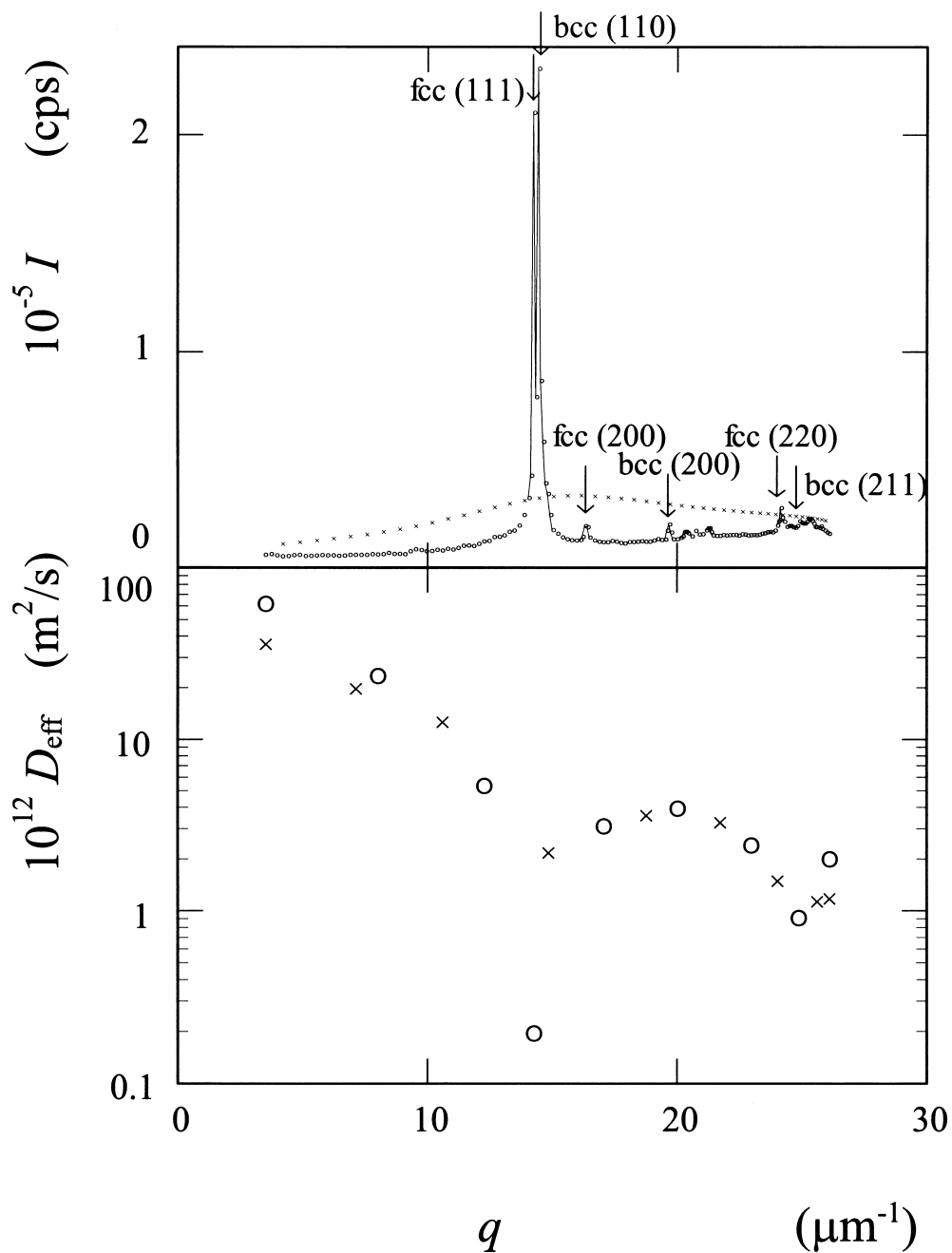


Fig. 2. Scattering intensity and diffusion coefficient as a function of scattering vector at 24°C , $\phi = 0.0049$, with resins for 7 days (O), without resins (X) (taken from OKUBO *et al.*, 1996).

8. Electro-Optics of Colloidal Crystals

Electro-optic effects such as Pockels and Kerr effects, where the change of refractive index of substances is induced by an applied electric field, have been extensively investigated recently. We studied a new-type of electro-optic device using the colloidal crystal systems (OKUBO, 1997c, 1999; STOIMENOVA and OKUBO, 1995, 1999; STOIMENOVA *et al.*, 1996). Since colloidal spheres are charged negatively and the expanded electrical

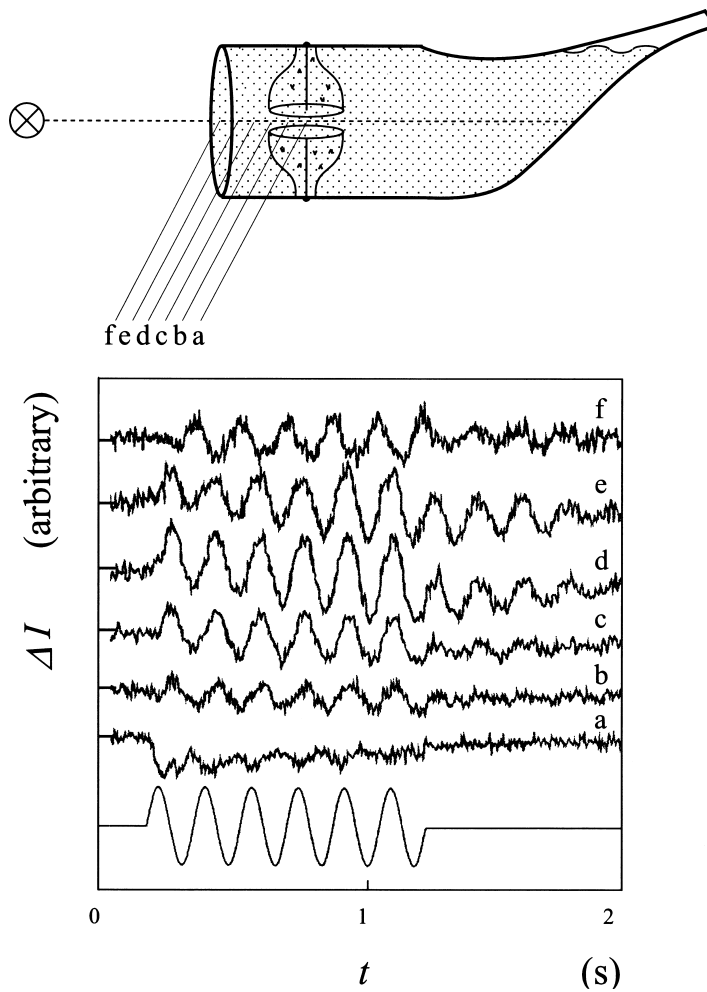


Fig. 3. Electric light-scattering measurements of colloidal crystals of silica spheres (103 nm in diameter) at 25°C. $f = 5.5$ Hz, $E = 40$ V, $\phi = 0.007$ (taken from OKUBO *et al.*, 1996).

double layers of the spheres are very soft, crystal lattice changes easily by the external electric fields (sine- and square-wave). The changes of the lattice spacing results in the electro-optic effects, because the Bragg distance is just in the range of light wavelength. We clarified several kinds of electro-optic effects using reflection spectroscopy. First, the peak wavelength shifted to longer and shorter wavelengths depending on the polarity of the electric fields. Second, waveforms in the intensity of the reflected light showed a significant phase difference from the applied field. This difference was significant for high field strengths and/or low frequencies. Third, amplitudes (a. c. component) in the responsive waveforms were large for the high electric field and/or low frequencies. Fourth, even outside area from the electrodes in between, strong signals were observed. This support strongly that the shear waves are induced by the applied electric field, like phonon. Fifth, harmonics especially the second-order harmonics was observed in high frequency and low electric field strength. Sixth, the standing waves and the characteristic frequencies were observed for colloidal crystal (STOIMENOVA *et al.*, 1996). Seventh, the resonance effect remained even after the applied a. c. field was off. Figure 3 demonstrates the effect measured by the electric light-scattering technique (STOIMENOVA *et al.*, 1996).

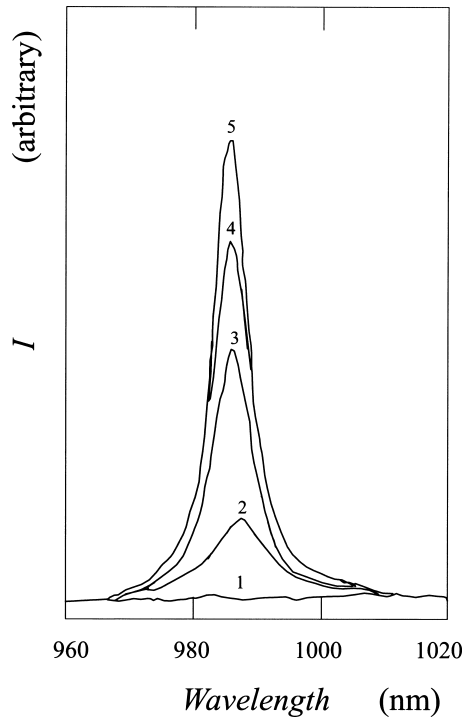


Fig. 4. Reflection spectra in the course of crystallization of colloidal silica spheres (110 nm in diameter) at 24°C, $\phi = 0.00179$, 17 days after suspension preparation with the resins. Curve 1: 5 s after mixing; 2: 15 s; 3: 20 s; 4: 25 s; 5: 600 s (taken from OKUBO and OKADA, 1997).

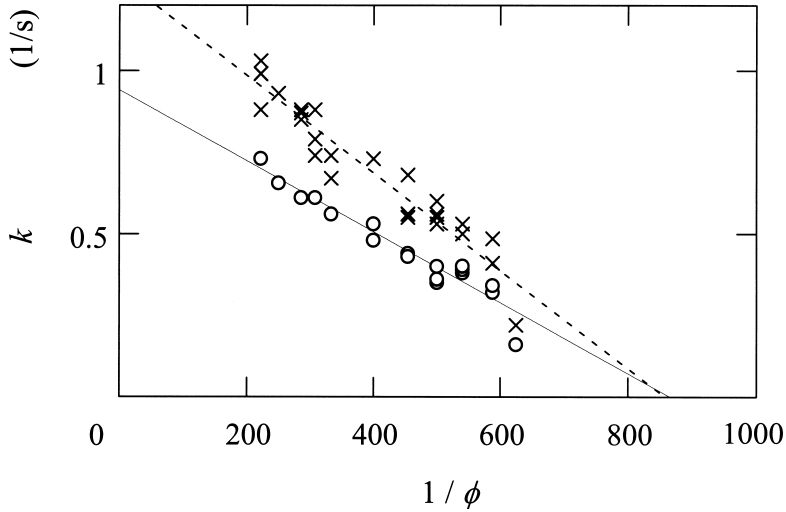


Fig. 5. Rate coefficients of colloidal crystallization plotted as a function of $1/\phi$ for silica spheres (110 nm in diameter) at 0G (○) and 1G (×) at 25°C, for fcc lattice (taken from OKUBO and ISHIKI, 1999).

9. Nucleation and Crystal Growth Processes

Colloidal crystallization has been analyzed from DLS measurements, from sharpening in the reflection peak, and from increase in the reflection peak intensity (OKUBO, 1997c; OKUBO and OKADA, 1997; OKUBO *et al.*, 1997). Typical reflection spectra in the course of crystallization are shown in Fig. 4. The induction periods were observed. During the induction periods the nucleation process is in progress. Kinetics of colloidal crystallization was the same as that of the classical diffusive crystallization theory including nucleation and crystal growth processes. The nucleation rates of colloidal crystallization were measured. The crystal growth rate of a crystal, v is given by:

$$v = v_{\infty} - v_{\infty} \phi_c / \phi$$

where v_{∞} , ϕ_c and ϕ are the maximum crystallization rate, critical sphere concentration of melting in volume fraction and sphere concentration, respectively. Kinetic analyses of colloidal crystallization in a sinusoidal electric field have been discussed by reflection spectroscopy (OKUBO and ISHIKI, 1999, 2000).

10. Colloidal Crystallization in Microgravity

Gravitational field is strong enough to change the structural and dynamic properties of colloidal crystals, including colloidal crystallization rates. The authors studied the colloidal crystallization in a microgravity achieved by the parabolic flights of a jet-aircraft. The stopped-flow cell system used for the reflection spectrum measurements.

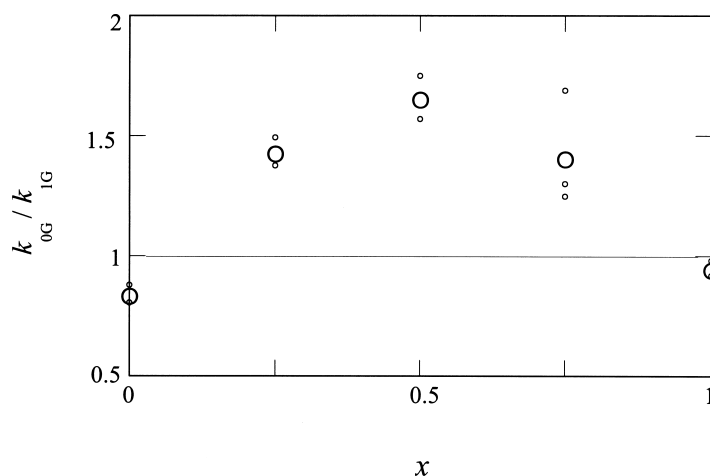


Fig. 6. Rate coefficient ratios (k_{0G}/k_{1G}) of colloidal alloy crystallization as a function of sphere volume fraction (x) in the polystyrene spheres (109 nm in diameter) + silica spheres (110 nm) at 25°C, total sphere concentration = 0.005 (taken from OKUBO *et al.*, 2000).

The growth rates of crystallization decreased by 25% in microgravity compared with normal gravity as shown by Fig. 5 (OKUBO *et al.*, 1999; TSUCHIDA *et al.*, 2000). One of the main causes for the retardation in microgravity is elimination of the downward diffusion of spheres, which enhances the inter-sphere collisions. No convection of the suspensions in microgravity was also or much more important than the elimination effect. The rates of colloidal alloy crystallization with the binary mixtures of different size or densities of spheres increased substantially in microgravity up to about 1.7 fold as shown in Fig. 6 (OKUBO *et al.*, 2000). The segregation effect is important in normal gravity for binary mixtures of colloid and powder science, i.e., large (or light) spheres are segregated upward and small (or heavy) ones downward. In microgravity such segregation should disappear and the homogeneous mixing should take place favorably, which leads fast alloy crystallization. It should be mentioned here that colloidal crystallization takes place by the packing model, i.e., alloy structure is determined by the condition whether the maximum packing density is achieved or not for a given ratio of the sphere sizes including surrounding electrical double layers.

REFERENCES

- OKUBO, T. (1986a) Transmitted light spectrum measurements, *J. Chem. Soc., Faraday Trans. 1*, **82**, 3175–3183.
 OKUBO, T. (1986b) Ordered solution structure of a monodispersed polystyrene latex as studied by the transmitted light spectrum method, *J. Chem. Soc., Faraday Trans. 1*, **82**, 3185–3196.
 OKUBO, T. (1986c) Ordered solution structure of a monodispersed polystyrene latex as studied by the reflection spectrum, *J. Chem. Soc., Faraday Trans. 1*, **82**, 3163–3173.
 OKUBO, T. (1987) Microscopic observation of ordered colloids in sedimentation equilibrium and important role of Debye-screening length. I. Heavy and monodispersed polystyrene type spheres (specific gravity = 1.50) in aqueous and aqueous methanol suspensions, *J. Chem. Phys.*, **86**, 2394–2399.

- OKUBO, T. (1988) Extraordinary behavior in the structural properties of colloidal macroions in deionized suspension and the importance of the Debye screening length, *Acc. Chem. Res.*, **21**, 281–286.
- OKUBO, T. (1989) Elastic modulus of crystal-like structures of deionized colloidal spheres in sedimentation equilibrium as studied by the reflection spectrum method, *J. Chem. Soc., Faraday Trans. 1*, **85**, 455–466.
- OKUBO, T. (1990a) Elastic modulus of crystal-like structures of deionized colloidal spheres in aqueous organic solvent mixtures, *J. Chem. Soc., Faraday Trans. 1*, **86**, 151–156.
- OKUBO, T. (1990b) Centrifugal compression of crystal-like structures of deionized colloidal spheres, *J. Am. Chem. Soc.*, **112**, 5420–5424.
- OKUBO, T. (1990c) Refractometric studies of “liquid-like” and “crystal-like” colloids in deionized solution, *J. Colloid Interface Sci.*, **135**, 294–296.
- OKUBO, T. (1991) Melting temperature of colloidal crystals of polystyrene spheres, *J. Chem. Phys.*, **95**, 3690–3697.
- OKUBO, T. (1992a) Giant single crystals of colloidal spheres in deionized and diluted suspension, *Naturwissenschaften*, **79**, 317–320.
- OKUBO, T. (1992b) Melting temperature of colloidal crystals of monodisperse silica spheres in ethanol-water and ethylene glycol-water mixtures, *Colloid Polym. Sci.*, **270**, 1018–1026.
- OKUBO, T. (1993a) Polymer colloidal crystals, *Prog. Polym. Sci.*, **18**, 481–517.
- OKUBO, T. (1993b) Large single crystals of colloidal silica spheres appearing in deionized and diluted suspension, *Colloid Polym. Sci.*, **271**, 190–196.
- OKUBO, T. (1994a) Colloidal single crystals of silica spheres in alcoholic organic solvents and their aqueous mixtures, *Langmuir*, **10**, 3529–3535.
- OKUBO, T. (1994b) Giant colloidal single crystals of polystyrene and silica spheres in deionized suspension, *Langmuir*, **10**, 1695–1702.
- OKUBO, T. (1994c) Phase diagram of ionic colloidal crystals, in *Macro-Ion Characterization. From Dilute Solutions to Complex Fluids* (ed. K. S. Schmitz), pp. 364–380, ACS Symp. Ser. 548, Am. Chem. Soc., Washington, D.C.
- OKUBO, T. (1997a) Structural relaxation time and rigidity of deionized suspensions of monodisperse polystyrene latex spheres, *J. Chem. Phys.*, **87**, 3022–3028.
- OKUBO, T. (1997b) Structural relaxation time and rigidity of ordered suspensions of monodispersed polystyrene latex spheres studied by spectrophotometric and conductance stopped-flow techniques, *J. Colloid Interface Sci.*, **117**, 165–171.
- OKUBO, T. (1997c) Recent advances in the kinetic and dynamic properties of colloidal crystals, *Current Topics in Colloid & Interface Sci.*, **1**, 169–193.
- OKUBO, T. (1999) Electro-optics of colloidal crystals as studied by the reflection spectroscopy, *Colloid & Surfaces A*, **149**, 431–441.
- OKUBO, T. and ISHIKI, H. (1999) Kinetic analyses of colloidal crystallization in an sinusoidal electric field as studied by reflection spectroscopy, *J. Colloid Interface Sci.*, **211**, 151–159.
- OKUBO, T. and ISHIKI, H. (2000) Kinetic analyses of colloidal crystallization in a wide range of sphere concentrations as studied by reflection spectroscopy, *J. Colloid Interface Sci.*, **228**, 151–156.
- OKUBO, T. and ISHIKI, H. (2001) Rigidity of colloidal alloys as studied by reflection spectroscopy in sedimentation equilibrium, *Colloid Polym. Sci.*, **279**, 571–578.
- OKUBO, T. and KIRIYAMA, K. (1997) Structural and dynamic properties in the complex fluids of colloidal crystals, liquids and gases, *J. Mol. Liq.*, **72**, 347–364.
- OKUBO, T. and OKADA, S. (1997) Kinetic analyses of the colloidal crystallization of silica spheres as studied by reflection spectroscopy, *J. Colloid Interface Sci.*, **192**, 490–496.
- OKUBO, T., KIRIYAMA, K., YAMAOKA, H. and NEMOTO, N. (1995) Dynamic properties of giant colloidal single crystals. Dynamic light scattering of monodispersed polystyrene spheres (192 nm in diameter) in deionized suspension, *Colloid & Surfaces A*, **103**, 47–58.
- OKUBO, T., KIRIYAMA, K., NEMOTO, N. and HASHIMOTO, H. (1996) Static and dynamic light-scattering of colloidal gases, liquids and crystals, *Colloid Polym. Sci.*, **274**, 93–104.
- OKUBO, T., OKADA, S. and TSUCHIDA, A. (1997) Kinetic study on the colloidal crystallization of silica spheres in the highly diluted and exhaustively deionized suspensions as studied by light-scattering and reflection spectroscopy, *J. Colloid Interface Sci.*, **189**, 337–347.

- OKUBO, T., TSUCHIDA, A., OKUDA, T., FUJITSUNA, K., ISHIKAWA, M., MORITA, T. and TADA, T. (1999) Kinetic analyses of colloidal crystallization in microgravity. Aircraft experiments, *Colloid & Surfaces A*, **160**, 311–320.
- OKUBO, T., TSUCHIDA, A., TAKAHASHI, S., TAGUCHI, K. and ISHIKAWA, M. (2000) Kinetics of colloidal alloy crystallization of binary mixtures of monodispersed polystyrene and/or colloidal silica spheres having different sizes and densities in microgravity using aircraft, *Colloid Polym. Sci.*, **278**, 202–210.
- OKUBO, T., ISHIKI, H., KIMURA, H., CHIYODA, M. and YOSHINAGA, K. (2002) Kinetics analysis of colloidal crystallization of silica spheres modified with polymers on their surfaces in acetonitrile, *Colloid Polym. Sci.*, **290**, 290–295.
- OTTEWILL, R. H. (1989) Colloid stability and instability: order disorder, *Langmuir*, **5**, 4–9.
- PIERANSKI, P. (1983) Colloidal crystals, *Contemp. Phys.*, **24**, 25–37.
- PUSEY, P. and VAN MEGEN, W. (1986) Phase behavior of concentrated suspension of nearly hard colloidal spheres, *Nature*, **320**, 340–342.
- ROBBINS, M. O., KREMER, K. and GREY, G. S. (1988) Phase diagram and dynamics of Yukawa systems, *J. Chem. Phys.*, **88**, 3286–3312.
- RUSSEL, W. B., SAVILLE, D. A. and SCHOWALTER, W. R. (1989) Colloid stability and instability: order disorder, in *Colloidal Dispersion*, Cambridge Univ. Press, Cambridge.
- SHINOHARA, T., YOSHIYAMA, T., SOGAMI, I., KONISHI, T. and ISE, N. (2001) Measurements of elastic constants of colloidal silica crystals by Kossel line analyses, *Langmuir*, **17**, 8010–8015.
- STOIMENOVA, M. and OKUBO, T. (1995) Electro-optic effects in colloidal crystals of spherical silica particles, *J. Colloid Interface Sci.*, **176**, 267–271.
- STOIMENOVA, M. and OKUBO, T. (1999) Electro-optical spectroscopy of colloidal systems, in *Surfaces of Nanoparticles and Porous Materials* (eds J. A. Schwarz and C. I. Contescu), pp. 103–124, Marcel Dekker, New York.
- STOIMENOVA, M., DIMITROV, V. and OKUBO, T. (1996) Electrically induced shear waves in colloidal crystals, *J. Colloid Interface Sci.*, **184**, 106–111.
- TSUCHIDA, A., TAGUCHI, K., TAKYO, E., YOSHIMI, H., KIRIYAMA, S., OKUBO, T. and ISHIKAWA, M. (2000) Microgravity experiments on colloidal crystallization of silica spheres in the presence of sodium chloride, *Colloid Polym. Sci.*, **278**, 872–877.
- WILLIAMS, R., CRANDALL, R. S. and WOJTOWICZ, P. J. (1976) Melting of crystalline suspensions of polystyrene spheres, *Phys. Rev. Lett.*, **37**, 348–350.